

PHYSICAL REVIEW LETTERS

VOLUME 27

20 DECEMBER 1971

NUMBER 25

Observation of H_β Satellites in the Presence of Turbulent Electric Fields

Charles C. Gallagher and Morton A. Levine

Air Force Cambridge Research Laboratories, Bedford, Massachusetts 01730

(Received 3 September 1971)

Satellites on either side of the H_β line of hydrogen are reported at a displacement from H_β corresponding to the plasma frequency ω_p and twice such frequency. This anomalous behavior of the H_β transition is correlated with an oscillating electric field associated with plasma turbulence.

Spectral line intensities and profiles, as influenced by local electric fields in a plasma, have been of recent interest both as a unique diagnostic tool to measure plasma parameters and as a problem of basic theoretical interest.¹⁻⁴ For instance, several papers reported the appearance of satellites near the 6632-Å (2^1P-3^1P) forbidden transition in neutral helium. These satellites are produced by electric fields, due to plasma oscillations, mixing the forbidden transition with the 6678-Å (2^1P-3^1D) allowed transition. The second-order Stark effect gives a two-photon process that results in emission at $\nu \pm \omega$, where ν is the frequency of the forbidden transition, and ω is the frequency of the time-varying electric field due to the plasma.

In this paper we report details of the observed profile of the H_β line in hydrogen, which is subject to first-order Stark effects, under the effect of high-frequency plasma fields. During plasma heating, the H_β exhibits satellites, arranged symmetrically about H_β and separated from the central line by ω_p and $2\omega_p$, where ω_p is the plasma frequency.

The observations were carried out in the Tormac plasma containment experiment, previously described.⁵ Plasma is created within a toroidal glass chamber 0.27 m in diameter. Subsequently, an H -centered⁶ (stabilized) pinch is produced, followed immediately by the application of a hexapole cusp magnetic field. The principal fields

rise in about 10 μ sec, during which time plasma density and temperature increase rapidly but uniformly to maximum values of approximately 10^{22} m⁻³ and 15×10^4 K. The fields decay slowly with the plasma exhibiting a containment time constant of about 200 μ sec.

Data were obtained by using a ten-channel polychromator⁷ which includes a 0.50-m Bausch and Lomb monochromator. Light enters the monochromator via a spot-to-line light guide which can be positioned to monitor the plasma light from within or outside the region of emission. Ten line-to-spot light guides, providing an effective resolution of 1 Å at the exit, transmit the desired wavelengths to the detection and recording instrumentation system. Line intensity profiles are plotted from oscillograph traces for any desired instant in the discharge period.

The profiles are corrected for instrumental errors. Then, electron density determinations are normally obtained from the shape of the Stark-broadened H_β profile using Hill's tabulation⁸ of the general results of Griem, *et al.* The comparisons are always made above the regions of any satellites that may be present. Temperatures are obtained from the ratio of the intensities of H_β to the surrounding continuum.

In addition to the spectroscopic system, instrumentation includes magnetic probes, a Rogowski coil which measures the plasma current, and a laser interferometer to provide additional elec-

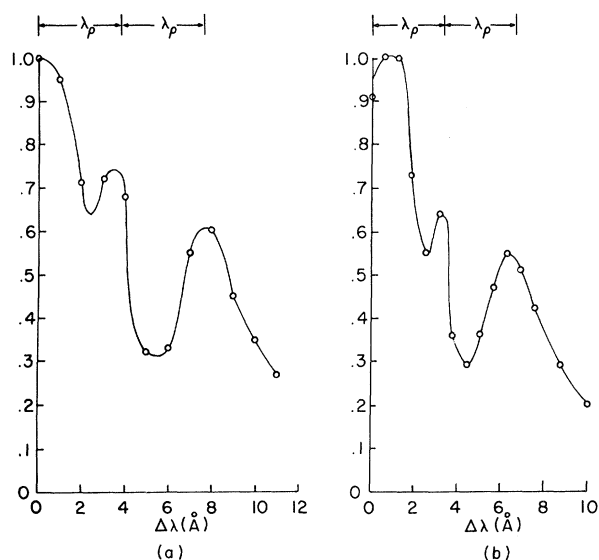


FIG. 1. H_{β} profiles on a relative intensity scale with wavelength increments measured from the line center. λ_p corresponds to the plasma frequency. Curves obtained using (a) polychromator and (b) individual shots.

tron density measurements.

Most studies of the plasma behavior are carried out at 100 mTorr pressure using hydrogen, but measurements at 30 mTorr pressure generally produce more marked anomalies in the H_{β} profiles. The anomalies occur only during ionization and heating of the plasma. Recently, a helium tracer has been added as a diagnostic aid, and profiles of the 6678- \AA allowed line, the associated forbidden line at 6632 \AA , and its satellites in helium have been observed under the same conditions as for the H_{β} profile.

Figures 1 and 2 show individual spectral profiles for approximately 5 μsec before the peaks of both electron density and magnetic fields. In each case, λ_p , the wavelength increment corresponding to the plasma frequency, is shown.

Profiles from separate series can only be compared to within a 1- μsec tolerance, a negligible factor for most of the discharge period, but not within the interval of satellite occurrence where the electron density is increasing rapidly (better than $10^{21} \text{ m}^{-3}/\mu\text{sec}$ for 100 mTorr). For this reason λ_p , for each of the H_{β} profiles shown, was calculated from the electron density based on the Stark broadening of that same profile. These electron densities were compatible with the laser interferometer measurements and with the densities based on Stark broadening but obtained outside the interval of turbulence.

The H_{β} profiles in Fig. 1 were obtained at 30

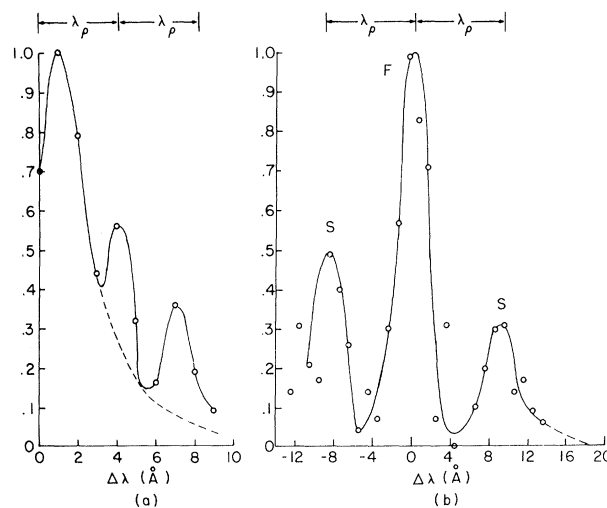


FIG. 2. (a) Folded H_{β} profile; (b) satellites (S) and 6632- \AA forbidden line (F) in helium tracer.

mTorr pressure. Only the lower wavelength halves of the profiles are shown because the profiles are symmetric about the line center. The data averages for the profile of Fig. 1(a) were obtained using the polychromator and several successive overlapping monochromator settings. λ_p corresponds to the density of $2.9 \times 10^{21} \text{ m}^{-3}$, obtained from the linewidth.

As a check against polychromator errors, Fig. 1(b) was obtained under the same conditions, but with only a single detector on the monochromator. This requires a large number of discharges over many monochromator settings. λ_p corresponds to $n = 2.2 \times 10^{21} \text{ m}^{-3}$.

Figure 2 shows both hydrogen and helium satellites obtained for 100 mTorr pressure. In Fig. 2(a), a typical H_{β} profile, λ_p corresponds to $3.4 \times 10^{21} \text{ m}^{-3}$. The dashed portion indicates the wings of the theoretical profile that was matched to the experimental profile above the region of the satellites. The temperature at this time is about $7 \times 10^4 \text{ K}$.

In the helium profile, Fig. 2(b), λ_p corresponds to $4.8 \times 10^{21} \text{ m}^{-3}$, the average electron density obtained from several H_{β} profiles for this time ($5 \pm 1 \mu\text{sec}$ before peak values). The close match between λ_p and the positions of the helium satellites provides additional confirmation of the values of electron densities based on Stark broadening.

The left or far satellite appears larger than the near satellite because it is superimposed on the wing of an unidentified, weak, impurity line which occurs just beyond the satellite.

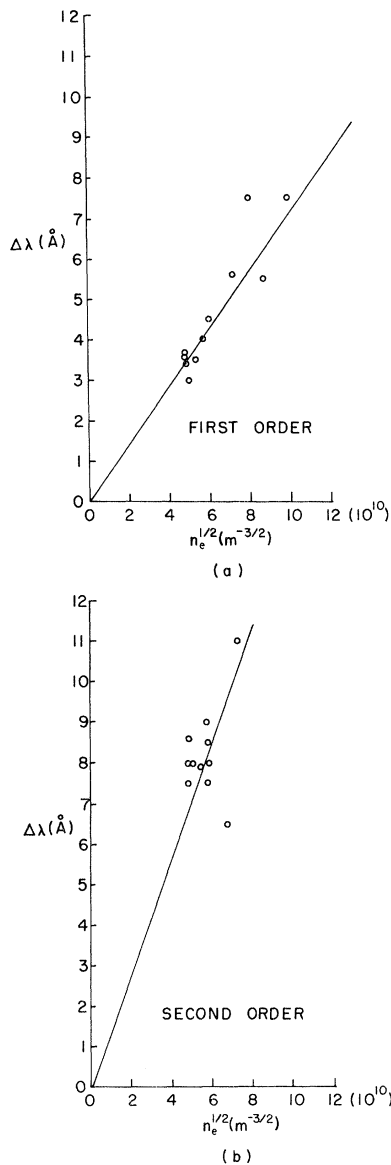


FIG. 3. Observed separations of satellites from the center of the H_{β} profile. Solid lines show predicted separations corresponding to (a) ω_p and (b) $2\omega_p$.

The H_{β} profiles are symmetric about the line center to within experimental error. This fact and the magnitude of λ_p rule out both impurity lines and the Doppler shifts as producing the observed anomalies.

Figure 3 shows the positions of the observed first- and second-order H_{β} satellites from several profiles as a function of $n^{1/2}$ for the simultaneous values of electron density n . Satellite positions from both the long- and short-wavelength wings of the H_{β} line are included. Inspection of Fig. 3 indicates that any deviations (e.g.,

in Figs. 1 and 2) lie within the range of experimental error.

Whereas it is possible to establish the electron density with reasonable confidence, it is much more difficult to determine the intensity of the oscillating electric field. The accuracy is limited both by the lower signal-to-noise ratio for the relatively weak satellite and forbidden lines and by the polychromator resolution and more difficult instrumental broadening corrections on the intense but very narrow allowed line profile. The most reliable value, near 10^7 V/m, is based on the ratio of the integrated intensities of the satellite to allowed line.¹

Using the measured intensities of the forbidden and allowed lines,¹ the intensity of the resultant field which produces the forbidden line was calculated to be roughly half that of the high-frequency field. This value is well in excess of the collisional field strength (which varies as $n^{2/3}$), thereby indicating the presence of low-frequency turbulence at that time.

The existence of low-frequency turbulence in the Tormac plasma during heating would appear to make suspect the electron density determinations based on the H_{β} profiles at this time. Even so, a close correlation among results from the various methods for electron density determination is noted.

Hydrogen satellites induced by oscillating electric fields were considered theoretically by Blokhintsev.⁹ In his theory, the intensity of the satellite associated with the p th harmonic of the applied frequency is proportional to the Bessel function squared, $J_p^2(x)$, where x varies as the field strength. For sufficiently strong fields, e.g., 10^7 volts/m, the second-order satellite can be expected to be more intense than the first-order satellite, with the exact ratio also a function of the strong static or low-frequency fields.¹⁰

In summary, in a helium-hydrogen plasma of about 5×10^{21} m⁻³ and temperature of 7×10^4 K a high-frequency plasma oscillation of close to 10^7 V/m was created. The oscillating electric field left the central structure of the H_{β} profile essentially unchanged but produced satellites, symmetrically positioned either side of the center of H_{β} and separated from the center by frequencies corresponding to the plasma frequency and twice the plasma frequency. The half-widths of these satellites are less than the half-width of the central line.

The authors wish to thank Robert Hargreaves and George Roberts who obtained much of the

data.

¹M. Baranger and B. Mozer, *Phys. Rev.* **123**, 25 (1961).

²H.-J. Kunze and H. R. Griem, *Phys. Rev. Lett.* **21**, 1048 (1968).

³N. Ben-Yosef and A. G. Rubin, *J. Quant. Spectrosc. Radiat. Transfer* **11**, 1 (1971).

⁴A. B. Berezin, L. V. Dubovoi, and B. V. Liublin, in *Proceedings of the Fourth International Conference on Plasma Physics and Controlled Nuclear Fusion Re-*

search, Madison, Wisconsin, 1971 (to be published).

⁵C. C. Gallagher, L. S. Combes, and M. A. Levine, *Phys. Fluids* **13**, 1617 (1970).

⁶M. A. Levine, L. S. Combes, W. Fitzsimmons, and S. Zimmerman, *Bull. Amer. Phys. Soc.* **3**, 39 (1958).

⁷L. S. Combes and C. C. Gallagher, *Appl. Opt.* **7**, 857 (1968).

⁸R. A. Hill, *J. Quant. Spectrosc. Radiat. Transfer* **7**, 401 (1967).

⁹D. Blokhintsev, *Phys. Z. Sowjetunion* **4**, 501 (1933).

¹⁰P. Bakshi, A. Cohn, and G. Kalman, to be published.

Polarized Electrons by Photoemission from Solid Alkalis

U. Heinzmann, J. Kessler, and B. Ohnemus

Physikalisches Institut der Universität Münster, Münster, Germany

(Received 10 November 1971)

We have observed spin polarization of photoelectrons emitted by solid alkali targets exposed to circularly polarized light. The polarization increases monotonically with increasing atomic number.

In earlier experiments¹⁻³ Fano's prediction⁴ of a polarization effect in photoionization of the alkalis was verified: Photoelectrons emitted by free alkali atoms exposed to circularly polarized light are highly spin polarized if the wavelength of the light falls within a broad spectral band near the ionization threshold. This polarization is due to the influence of spin-orbit interaction on photoionization.

It is the purpose of the present paper to report the first measurements on spin polarization of photoelectrons emitted by solid alkali targets exposed to circularly polarized light.

The apparatus used has been fully described in an earlier paper,³ the only major change being that the target was no longer an atomic beam. Instead, the alkali atoms were evaporated on a substrate in high vacuum at a rate of about 50 atomic layers per second.

The experimental results for cesium are given in Fig. 1. There are the following characteristic differences between these results and those for free cesium atoms: (1) The polarization maximum is shifted to longer wavelengths in the visible range, which makes the experiments very convenient. (2) The polarization is much lower. (3) The intensity obtained with the solid target is much higher.

Similar results were obtained for the other alkalis. For reasons of conciseness they are presented schematically in Fig. 2. The uncertainty of all the curves is given by the error bar in Fig.

2. It is the same for all targets. Within these error limits no polarization was found for Li and Na. For K a small polarization appeared. It increased as the atomic number became larger.

Whereas the earlier results for free alkali atoms were perfectly explained by Fano's theory, it is much more difficult to understand the present measurements. The similarity of the effect for free atoms and solid targets as well as the fact that the polarization increases with increasing atomic number, as does spin-orbit interaction, suggests that the polarization is caused by spin-orbit coupling. On the other hand, there is no appreciable spin-orbit interaction to be expected for the conduction electrons of the alkalis.

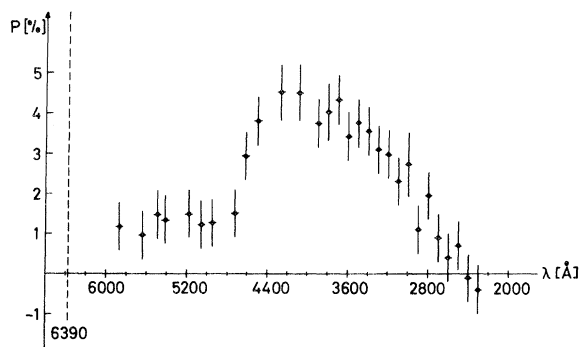


FIG. 1. Wavelength dependence of the polarization of photoelectrons produced by exposing solid cesium to circularly polarized light. Dashed line, ionization threshold.